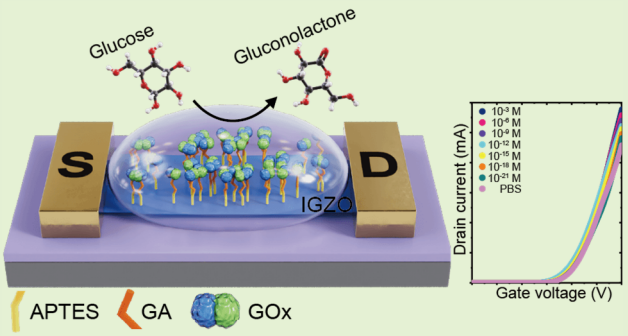
# Noninvasive and Ultrasensitive Glucose Detection via Electrolyte-Gated IGZO Thin-Film Transistors

Chuljin Hwang, Sungjun Park, and Dae Yu Kim

***Abstract*—Diabetes mellitus (DM) requires continuous glucose monitoring to avoid severe complications, yet conventional blood-based methods are invasive and unsuitable for frequent application. Tear fluid has emerged as an attractive alternative due to its noninvasive accessibility and rapid reflection of systemic glucose levels; however, the ultralow glucose concentration and complex matrix pose major analytical challenges. In the current study, we describe an ultrasensitive glucose sensor based on electrolyte-gated indium gallium zinc oxide thin-film transistors (IGZO-EGTFTs) functionalized with glucose oxidase (GOx). Stepwise surface modification was verified by atomic force microscopy (AFM) and contact angle analysis. The sensor exhibited a detection limit of 1 zM from a 1-$\mu$L sample, a linear range of 1 zM to 1 mM ($R^2$ = 0.993), and stable performance over 30 days. High selectivity against common tear interferents was also observed. These findings establish IGZO-EGTFTs as a promising platform for noninvasive and reliable tear-based glucose monitoring at the point of care.**




***Index Terms*— Electrolyte-gated thin-film transistor (TFT), glucose sensor, indium gallium zinc oxide electrolyte-gated TFT (IGZO-EGTFT), metal oxide (MOx) sensor.**

## I. Introduction

DIABETES mellitus (DM) is a chronic metabolic disorder that poses a significant threat to global health [1], [2]. Inadequate glycemic control can result in acute hypoglycemic episodes and elevate the risk of long-term complications, underscoring the critical need for accurate and timely glucose monitoring [3], [4]. Currently, glucose measurement relies on strip-based glucometers, which require intermittent capillary blood sampling via multiple daily finger pricks [5], [6], [7]. While these devices are commonly used, they are invasive and may cause discomfort and carry risks, such as local infection and tissue damage, particularly for individuals with impaired wound healing. Such drawbacks often contribute to reduced patient compliance [8], [9]. These issues have prompted the advancement of noninvasive glucose sensing platforms to enable real-time, blood-free monitoring and improve patient comfort and usability.

For noninvasive glucose monitoring, alternative biological fluids, such as saliva [10], [11], urine [12], [13], sweat [14], [15], and tears [16], [17], have been explored. Tears, in particular, have garnered significant interest due to their ease of collection, minimal discomfort during sampling, relatively low infection risk, and rapid glucose responsiveness attributed to the "plasma leakage" phenomenon [18], [19], [20]. Although a quantifiable correlation between blood and tear glucose concentrations has been established, glucose levels in tear fluid are approximately 30–50 times lower than those in blood [18], [21], [22], [23]. These ultralow concentrations underscore the critical need for highly sensitive and robust sensing technologies capable of accurately detecting glucose concentrations within tear fluid.

Received 27 January 2026; accepted 30 January 2026. Date of publication 19 February 2026; date of current version 14 May 2026. This work was supported in part by the National Research Foundation of Korea (NRF) under Grant RS-2018-NR031065, Grant RS-2024-00460600, and Grant RS-2025-00559359; in part by Korea Institute for Advancement of Technology (KIAT) through Korean Government [Ministry of Trade, Industry and Energy (MOTIE)] (HRD Program for Industrial Innovation) under Grant RS-2022-KI002581; and in part by the BK21 Four Program through the Ministry of Education (MOE, Korea). The associate editor coordinating the review of this article and approving it for publication was Dr. Sunipa Roy. *(Corresponding authors: Sungjun Park; Dae Yu Kim.)*

Chuljin Hwang is with the Department of Electrical and Computer Engineering, Center for Sensor Systems, Inha University, Incheon 22212, Republic of Korea (e-mail: aki@inha.ac.kr).

Sungjun Park is with the Department of Electrical and Computer Engineering, Ajou University, Suwon 16499, Republic of Korea (e-mail: sj0223park@ajou.ac.kr).

Dae Yu Kim is with the Department of Electrical and Computer Engineering, Center for Sensor Systems, Inha Research Institute for Aerospace Medicine, Inha University, Incheon 22212, Republic of Korea (e-mail: dyukim@inha.ac.kr).

This article has supplementary downloadable material available at https://doi.org/10.1109/JSEN.2026.3661008, provided by the authors.

Digital Object Identifier 10.1109/JSEN.2026.3661008

© 2026 The Authors. This work is licensed under a Creative Commons Attribution 4.0 License.
For more information, see https://creativecommons.org/licenses/by/4.0/

To address this challenge, metal oxide (MOx) semiconductor thin-film transistors (TFTs) have emerged as a promising sensing platform for biomolecular detection due to distinct features, including signal amplification, scalable fabrication, and chemical stability [24], [25], [26], [27], [28], [29]. Among the various MOx materials, zinc oxide (ZnO), indium tin oxide (ITO), indium zinc oxide (IZO), and indium gallium zinc oxide (IGZO) have been extensively investigated as potential active channel materials for electrolyte-gated biosensors, each offering distinct electrical properties. ZnO exhibits high intrinsic carrier mobility but is often affected by grain-boundary variability inherent to its nanocrystalline structure. In contrast, ITO and IZO demonstrate greater susceptibility to electrolyte-induced ion diffusion, which can lead to interfacial charge screening and increased electrical noise during electrolyte-gated sensing [30], [31]. IGZO, with its amorphous channel architecture, provides enhanced electronic uniformity and robustness in aqueous environments, supporting stable, reproducible electrical signal transduction [32], [33]. Leveraging these material-level advantages, IGZO-based electrolyte-gated TFTs (EGTFTs) have garnered significant attention for their stability in aqueous environments, low-voltage operation (<1 V), rapid transient response, high ON/OFF current ratio, simple surface functionalization, and the capacity to amplify and convert biological signals into measurable electrical outputs [34], [35], [36], [37], [38].

For instance, Bhatt et al. [39] developed an IGZO-based electrolyte-gated field-effect transistor (EGFET) for prostate-specific antigen (PSA) detection. In this device, anti-PSA antibodies were immobilized on the IGZO surface using a 3-aminopropyltriethoxysilane (APTES)–glutaraldehyde (GA) linkage, and a concentration-dependent decrease in drain current was observed across a range from 1 pg/mL to 10 ng/mL in phosphate-buffered saline (PBS). Additionally, Zhang et al. [40] reported an IGZO-based FET biosensor functionalized with a paperclip-shaped nucleic acid probe, facilitating label-free detection of single-nucleotide polymorphisms in severe acute respiratory syndrome coronavirus 2 RNA. This sensor enables rapid identification of viral variants within 15 min, achieving a detection limit of 0.03 copies $\mu L^{-1}$ and discrimination accuracy of 97.1% in simulated clinical samples.

However, quantitative glucose detection in tears remains challenging due to the presence of multiple biomolecules, such as $\beta$-casein, dopamine (DA), uric acid, albumin, and lactoferrin, which may interfere with selectivity. Furthermore, the limited tear volume available for analysis and rapid fluctuations in glucose concentration caused by evaporation impose additional constraints on sensor sensitivity. These challenges underscore the need for sensing platforms with ultrahigh sensitivity, rapid response, and high specificity to enable accurate detection of trace glucose levels from small volumes of tear fluid.

This study presents the development of a glucose sensor utilizing IGZO electrolyte-gated TFTs (IGZO-EGTFTs) functionalized with glucose oxidase (GOx) for ultrasensitive and real-time glucose monitoring. The sophisticated surface functionalization process was investigated using atomic force microscopy (AFM) and water contact angle (WCA) measurements. Collectively, the findings of this study underscore the potential of IGZO-EGTFTs as a powerful platform for noninvasive, tear-based glucose monitoring.

## II. Materials and Methods

### A. Materials

Indium nitrate hydrate [$In(NO_3)_3 \cdot xH_2O$], gallium nitrate hydrate [$Ga(NO_3)_3 \cdot xH_2O$], zinc acetate dihydrate [Zn(CH3COO)2·2 H2O], and 2-methoxyethanol were purchased from Sigma–Aldrich (St. Louis, MO, USA) and used without further purification. Human serum albumin (HSA; A1653), human lactoferrin (L1294), D-(+)-glucose (G7528), GOx from *Aspergillus niger* (G7141), $\beta$-casein from bovine milk (C6905), and bovine serum albumin (BSA; 10 775 835 001) were also purchased from Sigma–Aldrich (St. Louis, MO, USA). Moreover, 3-APTES and GA were purchased from Sigma–Aldrich and stored in a dry, ventilated place. PBS was purchased from Samchun (Seoul, South Korea) and used as the electrolyte medium. Deionized (DI) water (18 MΩ cm, 25 °C) was used throughout. Polydimethylsiloxane (PDMS) prepolymer (Sylgard 184 A) and curing agent (Sylgard 184B) were obtained from Dow Corning (Shanghai, China).

### B. IGZO Precursor Synthesis

The IGZO precursor solution was prepared by dissolving $In(NO_3)_3 \cdot xH_2O$, $Ga(NO_3)_3 \cdot xH_2O$, and $Zn(CH_3COO)_2 \cdot 2H_2O$ in 2-methoxyethanol to a final concentration of 0.1 M and at an In:Ga:Zn molar ratio of 0.1:0.15:0.0275, with stirring at 60 °C for 4 h. The resulting solution was filtered using a 0.2-$\mu$m hydrophobic polytetrafluoroethylene (PTFE) syringe membrane before use.

### C. Fabrication Process

IGZO-EGTFTs were fabricated on heavily boron-doped silicon wafers featuring a 300-nm thermally grown, $SiO_2$ insulating layer. The source and drain (S/D) electrodes were patterned using conventional photolithography, followed by sequential deposition of titanium (10 nm) and gold (50 nm) via electron-beam evaporation. Prior to active layer deposition, the substrate surface was treated with oxygen plasma (Femto Science, Korea) at 100 W for 10 min to enhance wettability. The IGZO channel layer was formed by spin-coating a sol–gel-derived IGZO precursor solution at 4000 r/min for 30 s, followed by thermal annealing at 400 °C for 1.5 h to produce a densified oxide semiconductor. The IGZO layer was patterned using photolithography and wet etching to define the active region. Epoxy-based SU-8 3008 was used for passivation, leaving only the sensing area exposed. The detailed fabrication process is presented in Fig. S1.

### D. Surface Functionalization for Detecting Glucose

The IGZO surface was first treated with oxygen plasma (60 W, 1 min) to introduce hydroxyl groups, increasing surface hydrophilicity. For silanization, a 10% (v/v) APTES solution in ethanol was prepared and vortexed for 3 min.

The IGZO substrate was immersed in the solution for 17 h, rinsed with DI water, and dried under nitrogen flow. This process introduced amine ($-NH_2$) functional groups onto the IGZO surface. Subsequently, the APTES-modified IGZO surface was functionalized with a GA solution by drop-casting, enabling covalent linking of aldehyde groups with IGZO surface amines. For enzyme immobilization, GOx was dissolved in PBS at 10 mg/mL and vortexed for 2 min until fully dissolved. The GA-functionalized IGZO surface was incubated in the GOx solution to allow covalent immobilization via Schiff base formation.

### E. Surface Characterization

Surface morphology and chemical composition were evaluated using AFM and WCA measurements. AFM imaging was performed in noncontact mode using an NX10 system (Park Systems, Republic of Korea), equipped with a probe featuring a resonance frequency of 330 kHz and a spring constant of 42 N/m. Images were acquired across a 5 × 5 $\mu$m scan area to evaluate nanoscale surface features.

Surface wettability was characterized by WCA measurements. A 10-$\mu$L droplet of DI water was placed on the sample surface, and side-view images were captured using a digital camera (Ace 2000–165 $\mu$m, Basler, Germany). Contact angles were calculated using ImageJ, and the results were averaged across three independent measurements. All measurements were performed at 25 °C and 30%–35% relative humidity.

### F. Electrical Characteristics

For electrical characterization of the IGZO-EGTFTs, PBS was used as the liquid gate electrolyte. A CHI111 Ag/AgCl reference electrode (RE; CH Instruments) with a 1-M KCl inner filling was used as the gate electrode, immersed in a 20-$\mu$L electrolyte droplet on a single cell containing 20 EGTFTs within a 1.5 × 1.5 $cm^2$ area. All potentials referenced the Ag/AgCl electrode. Electrical measurements were performed at room temperature using a Keithley 2602B dual-channel source meter (Keithley, Cleveland, OH, USA) with a sweep rate of 1000 mV/s under ambient conditions in a dark box. After each measurement cycle, the device was thoroughly rinsed with DI water and dried under a nitrogen flow. The normalized response (NR) of the sensor was calculated using the following equation:

$$\mathrm{NR} = \left| \frac{I_D - I_O}{I_O} \right| \tag{1}$$

where $I_O$ and $I_D$ are the drain currents of the IGZO-EGTFTs before and after treatments, respectively.

## III. Results and Discussion

### A. Surface Characterization

Fig. 1(a) illustrates the sequential surface functionalization steps employed to immobilize GOx on the IGZO substrate for glucose detection. The functionalization process began with oxygen plasma treatment to introduce hydroxyl groups on the IGZO surface, followed by silanization using APTES as the first crosslinker, which formed covalent Si–O–Si bonds with surface −OH groups, generating a self-assembled monolayer with terminal amine groups. Subsequently, GA was used as the second crosslinker to react with the surface amine groups of APTES, introducing aldehyde functionalities that served as anchoring points for enzyme immobilization. Finally, GOx was covalently attached via Schiff base formation between aldehyde groups and the enzyme's lysine residues, resulting in a stable and bioactive sensing interface [41].

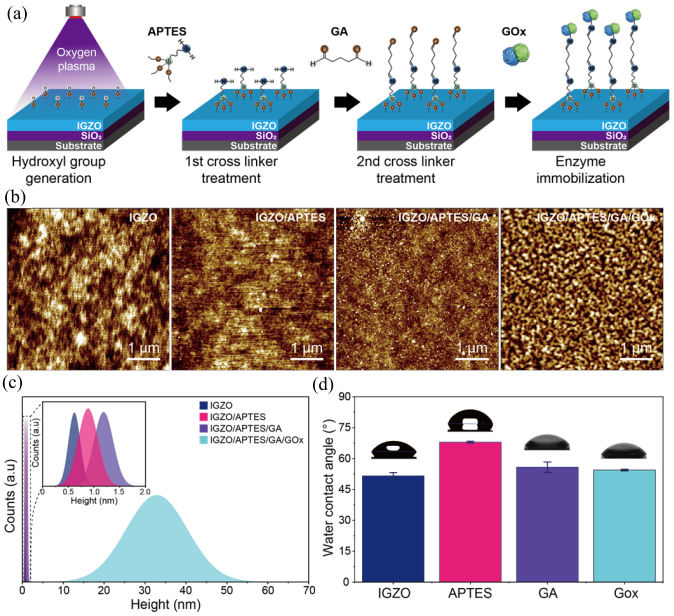



Fig. 1. Surface functionalization of the IGZO surface for glucose detection. (a) Schematic illustration of the stepwise surface functionalization process and (b) corresponding AFM images for enzyme immobilization on the IGZO surface: hydroxyl group generation via oxygen plasma treatment; silanization with 3-APTES as the first crosslinker; GA treatment as the second crosslinker; and subsequent immobilization of GOx. (c) Height distribution profiles extracted from AFM data. (d) Static WCA measurements and photographs showing changes in surface wettability through each surface functionalization step.

To investigate each step of the surface functionalization process, AFM and WCA measurements were sequentially performed. The IGZO surface exhibited smooth and compact morphology, with a root mean square (rms) roughness (Rq) of approximately 0.181 nm [Fig. 1(b)]. Following APTES treatment, the Rq increased to 0.255 nm, indicating successful organosilane monolayer formation. Subsequent GA functionalization introduced additional molecular crosslinkers, further increasing the surface roughness to 0.314 nm. Upon GOx immobilization, granular features became apparent, and the Rq markedly increased to 7.602 nm, representing a 7.288 nm increase over the APTES/GA-modified surface, indicating substantial enzyme immobilization. These trends were further supported by height distribution profiles from AFM analysis [Fig. 1(c)], which exhibited a gradual shift and broadening in surface roughness through each modification step, most notably after GOx immobilization. This provides strong evidence of a controlled and progressive surface functionalization process.

The surface wettability before and after functionalization was evaluated by WCA measurements [Fig. 1(d)]. The IGZO

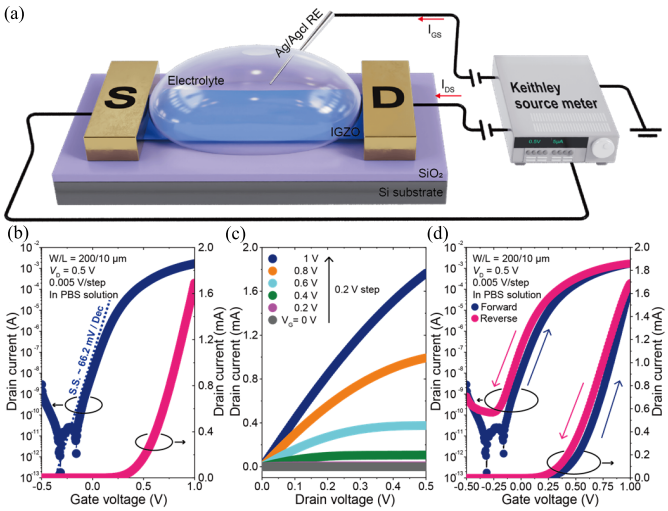



Fig. 2. Electrical characteristics of IGZO-EGTFTs. (a) Schematic illustration of the device structure under liquid-gated conditions, showing the measurement configuration with the electrolyte and Ag/AgCl reference electrode. (b) Transfer characteristics ($I_{DS}$ versus $V_{GS}$) measured at $V_{DS}$ = 0.5 V ($V_{GS}$ = −0.5–1 V). The device shows the typical n-type behavior with a subthreshold slope (SS) of 66.8 mV/dec. (c) Output characteristics ($I_{DS}$ versus $V_{DS}$) curves of the IGZO-EGTFT at gate voltages ranging from 0 to 1 V in 0.2 V increments. (d) Counterclockwise hysteresis curve between the forward and backward gate voltage sweeps.

surface exhibited moderate hydrophilicity, with a contact angle of 51.6°, which increased to 67.9° after APTES functionalization. This increase was primarily attributed to the reduced surface polarity resulting from nonpolar alkyl silane groups. After GA treatment, the WCA decreased to 55.8°, consistent with previously reported values for GA-modified surfaces [37]. Following GOx immobilization, the WCA decreased slightly to 54.4°, indicating enhanced surface hydrophilicity. This change was attributed to the presence of polar functional groups, including hydroxyl, carboxyl, and amino groups, as well as hydrophilic moieties exposed on the enzyme layer.

### B. Electrical Characterization of IGZO-EGTFTs

The IGZO-EGTFTs adopted a top-gate/bottom-contact structure [Fig. 2(a)]. The device featured an IGZO channel partially patterned and exposed between the Au source and drain electrodes on a Si substrate, with a channel width and length of 200 and 10 $\mu$m, respectively ($W/L$ = 20, Fig. S2). An Ag/AgCl RE was immersed in the electrolyte covering the IGZO channel to apply the gate voltage during operation. The applied gate bias induced ionic accumulation near the IGZO–electrolyte interface, leading to electric double layer (EDL) formation comprising compact inner and outer Helmholtz layers. Due to its nanometer-scale thickness, the EDL exhibits high capacitance, enabling strong gate coupling and effective device modulation at low operating voltages [42], [43].

Before evaluating the glucose detection capacity of IGZO-EGTFTs, their intrinsic n-type transistor characteristics were examined. The transfer ($I_D$ versus $V_G$) characteristics of IGZO-EGTFT revealed exceptional on/OFF current ratios (Ion/Ioff) exceeding $10^{10}$ at $V_G$ from −0.5 to 1 V [Fig. 2(b)]. Additionally, the consistent gate-controlled transfer characteristics were maintained across drain voltages ($V_D$ = 0.1–0.5 V; Fig. S3). The output characteristics exhibited a linear region below the pinch-off voltage, indicating ohmic contact between the IGZO channel and Au source/drain electrodes [Fig. 2(c)]. Moreover, the transfer curves under forward and reverse gate sweeps exhibited negligible counterclockwise hysteresis [Fig. 2(d)]. This suggested that interfacial and bulk trap states in the IGZO layer remained electrically stable at the applied gate voltage sweep rate.

To evaluate electrical performance across devices, the transconductance (gm), subthreshold swing (SS), and threshold voltage ($V_{TH}$) were extracted from the transfer curves of 20 devices (Fig. S4). The average maximum gm, SS, and $V_{TH}$ were 3.896 mS, 66.187 mV/dec, and 0.120 V, respectively, demonstrating consistent switching behavior and reliable gate modulation.

Furthermore, operational stability under prolonged electrical bias was evaluated by monitoring the drain current ($I_{DS}$) as a function of time under fixed bias conditions ($V_{GS}$ = +1 V and $V_{DS}$ = +0.5 V). $I_{DS}$ remained relatively constant over a continuous measurement interval of $10^3$ s (Fig. S5), demonstrating the robustness of the IGZO channel with no observable current degradation. This period of demonstrated stability sufficiently encompasses the typical settling time required for reliable signal acquisition in biosensing measurements, thereby supporting its suitability for practical sensing operations [44].

### C. Sensitive, Real-Time, and Selective Glucose Detection

To evaluate the feasibility of IGZO-EGTFTs for glucose detection, sensing mechanisms and electrical characterization were evaluated, including sensitivity, selectivity, and real-time operation. The IGZO-EGTFT glucose sensor operates based on a cascade of biochemical and electrochemical reactions that transduce glucose concentration into an electrical signal [Fig. 3(a)]. GOx, covalently immobilized on the surface of the IGZO channel, catalyzes D-glucose oxidation to D-glucono-1,5-lactone and hydrogen peroxide ($H_2O_2$) in the presence of molecular oxygen, as indicated in the following equation:

$$D\text{-Glucose} \rightarrow D\text{-Glucono} - 1,\ 5 - \text{lactone} + H_2O_2. \tag{2}$$

The generated $H_2O_2$ is then electrochemically oxidized under an applied gate voltage at the gate–electrolyte interface, producing proton ions and electrons [45]

$$H_2 \rightarrow 2H^+ + O_2 + 2e^-. \tag{3}$$

Proton concentration increases the regulation of the local electrostatic environment at the interface between the electrolyte and IGZO surface, modulating the surface potential. This change, driven by glucose-dependent enzymatic proton generation, induces a shift in threshold voltage, which is transduced into a measurable change in drain current [46]. This mechanism was experimentally verified by evaluating the electrical response of IGZO-EGTFTs under controlled pH environments, simulating the effect of proton accumulation.

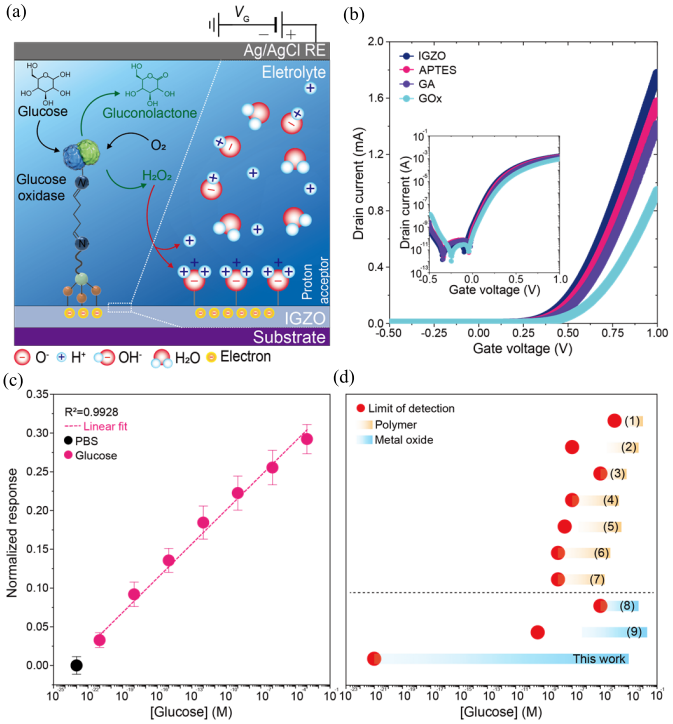



Fig. 3. Electrical characterization of the IGZO-EGTFT-based glucose sensor. (a) Schematic illustration of the sensing mechanism for glucose detection using the IGZO-EGTFTs. (b) Transfer curves of the device at each functionalization step: IGZO, 3-APTES treatment, GA treatment, and GOx-immobilization on the IGZO surfaces. (c) Calibration curve of drain current ($I_D$) versus glucose concentration (1 zM–1 mM) in 0.01× PBS, showing high linearity ($R^2 = 0.9928$). (d) Overview of sensing performance, including the LOD and detection range for various sensors based on polymer and MOx transistors, summarized from the data in Table S1.

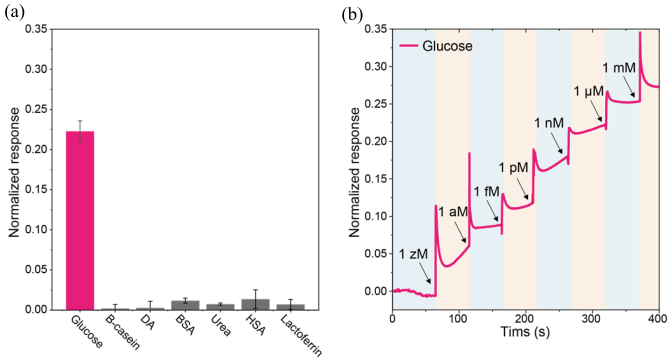



Fig. 4. Selectivity and sensitivity of the glucose biosensor IGZO-EGTFT. (a) Selectivity analysis of the sensor for glucose and potential interfering biomolecules, including $\beta$-casein, DA, BSA, urea, HSA, and lactoferrin. (b) Real-time monitoring of the NR values in response to glucose addition from 1 zM to 1 mM.

Decreasing the pH from 8 to 4 induced a progressive negative shift in threshold voltage, indicating increased carrier density of the IGZO channel due to enhanced surface protonation [Fig. S6(a)]. To evaluate the stability of this proton-mediated modulation, threshold voltage shifts were applied over multiple pH cycling steps, demonstrating a fully reversible and consistent response [Fig. S6(b)]. For statistical validation, the same pH cycling protocol was applied to 20 independent devices, demonstrating reproducible electrostatic behavior.

Fig. 3(b) presents the representative transfer characteristics of the IGZO-EGTFTs in accordance with sequential surface functionalization with APTES (first crosslinker), GA (second crosslinker), and GOx. At each functionalization step, a progressive decrease in drain current and a positive shift in threshold voltage were observed. These electrical shifts were attributed to the chemical reaction between the IGZO surface and the immobilized molecules, which modulate the interfacial charge environment. This consistent trend supports the successful stepwise assembly of functional layers through surface chemical reactions.

After surface functionalization, the IGZO-EGTFT sensor was assessed for its glucose detection capabilities. The device demonstrated a linear response in NR values across the $10^{-21}$–$10^{-3}$ M concentration range, displaying a strong correlation with glucose concentration [$R^2 = 0.9928$; Figs. 3(c) and S7]. To benchmark analytical performance, the limit of detection (LOD) and sensing range were compared with previously reported glucose sensors based on polymeric and MOx transistors. The IGZO-EGTFTs achieved a significantly lower LOD in the zM, which was 11 orders of magnitude lower than previously reported polymer and MOx transistor configurations, while maintaining a broad and linear detection range [Fig. 3(d), Table S1].

The ultralow LOD of the IGZO-EGTFT sensor is attributed to three key design features. First, the wide IGZO channel ($200 \times 10\ \mu$m) provides an enlarged sensing interface, increasing the probability of molecular interactions. Second, electrolyte gating enables direct surface potential modulation at the IGZO–electrolyte interface, where protons from enzymatic glucose oxidation modulate the channel current, allowing high sensitivity even in microliter-scale samples. Third, the sophisticated surface functionalization for immobilizing GOx on the IGZO channel ensures that even minute concentrations of glucose can trigger detectable proton generation.

The selectivity of the IGZO-EGTFT glucose sensor was evaluated by monitoring the NR values in real time following sequential additions of glucose and common tear components, such as $\beta$-casein, DA, BSA, uric acid, HSA, and lactoferrin [47], [48], [49], [50]. The sensor exhibited negligible responses to all interfering species, while its NR values changed in a glucose concentration-dependent manner [Fig. 4(a)].

To further assess its practical utility for continuous glucose monitoring, real-time drain current measurements were performed under sequential glucose addition in vitro. In this experiment, the drain current ($I_{DS}$) was continuously monitored under fixed source–drain ($V_{DS}$) and gate ($V_{GS}$) voltages as glucose was incrementally introduced into the electrolyte [Fig. 4(b)]. $I_{DS}$ exhibited stepwise increases that corresponded with higher glucose concentrations ranging from 1 zM to 1 mM.

Finally, the long-term stability of the sensor was evaluated after immobilizing GOx. The NR value was measured in glucose solutions every five days over a 30-day period. Between measurements, the sensors were stored under controlled conditions to preserve the IGZO surface integrity and enzymatic

activity. After 30 days, the sensor retained 92.91% of its initial NR values, demonstrating good stability (Fig. S8). This performance was attributed to the robust GOx immobilization on the IGZO surface, which maintained enzymatic activity during storage.

Additionally, sensor reproducibility was assessed across seven independently fabricated IGZO-EGTFT devices functionalized with GOx over 30 days. The RSD for 1-mM glucose was 3.94%, demonstrating excellent reproducibility (Fig. S9). Collectively, these results demonstrate that the IGZO-EGTFT sensor represents a reliable platform for sustained and precise glucose detection under practical usage conditions.

## IV. Conclusion

In summary, an ultrasensitive, real-time glucose sensor was developed based on IGZO-EGTFTs. Comprehensive surface characterization using AFM and WCA measurements verified the uniform immobilization of APTES, GA, and GOx on the IGZO surface, establishing a robust sensing interface. The sensor achieves an ultralow LOD of 1 zM and a wide linear detection range from $10^{-21}$ to $10^{-3}$ M ($R^2 = 0.9928$), surpassing the performance of previously reported glucose sensors. Additionally, the sensor exhibits good stability over time, making it a viable option for consistent and dependable glucose sensing in real-world applications. Furthermore, it enables reliable sensing in microliter-scale sample volumes, highlighting its compatibility with tear fluid-based glucose monitoring. Finally, the sensor demonstrates long-term operational stability over 30 days without noticeable degradation in detection accuracy, further demonstrating its potential as a robust tear glucose sensor.

Collectively, this study not only demonstrates highly sensitive, reliable, and quantitative glucose detection but also offers a promising diagnostic approach for noninvasive glucose monitoring and early intervention in diabetes management, supported by stable operation in complex biological environments and under minimal sample conditions.

## Author Contributions

Chuljin Hwang: design of experiment, electrical characterization, methodology, data analysis, and writing. Sungjun Park: writing review. Dae Yu Kim: project administration and writing review.

## Declaration of Competing Interests

The authors declare that they have no known competing financial interests or personal relationships that could have appeared to influence the work reported in this article.

## References


[1] American Diabetes Association, "Diagnosis and classification of diabetes mellitus," *Diabetes Care*, vol. 32, no. 1, pp. S62–S67, Jan. 2009, doi: 10.2337/dc09-S062.

[2] S.-H. Lee, S.-Y. Park, and C. S. Choi, "Insulin resistance: From mechanisms to therapeutic strategies," *Diabetes Metabolism J.*, vol. 46, no. 1, pp. 15–37, Jan. 2022, doi: 10.4093/dmj.2021.0280.

[3] T. Klupa et al., "Expanding the role of continuous glucose monitoring in modern diabetes care beyond type 1 disease," *Diabetes Therapy*, vol. 14, no. 8, pp. 1241–1266, Aug. 2023, doi: 10.1007/s13300-023-01431-3.

[4] B. Giri, S. Dey, T. Das, M. Sarkar, J. Banerjee, and S. K. Dash, "Chronic hyperglycemia mediated physiological alteration and metabolic distortion leads to organ dysfunction, infection, cancer progression and other pathophysiological consequences: An update on glucose toxicity," *Biomed. Pharmacotherapy*, vol. 107, pp. 306–328, Nov. 2018, doi: 10.1016/j.biopha.2018.07.157.

[5] T. K. Mathew, M. Zubair, and P. Tadi, "Blood glucose monitoring," in *StatPearls*. Treasure Island, FL, USA: StatPearls Publishing, 2025. [Online]. Available: http://www.ncbi.nlm.nih.gov/books/NBK555976/

[6] G.-J. Eerdekens, S. Rex, and D. Mesotten, "Accuracy of blood glucose measurement and blood glucose targets," *J. Diabetes Sci. Technol.*, vol. 14, no. 3, pp. 553–559, Feb. 2020, doi: 10.1177/1932296820905581.

[7] A. Nakhleh and N. Shehadeh, "Hypoglycemia in diabetes: An update on pathophysiology, treatment, and prevention," *World J. Diabetes*, vol. 12, no. 12, pp. 2036–2049, Dec. 2021, doi: 10.4239/wjd.v12.i12.2036.

[8] J. Chung, H. So, Choi, and T. K. S. Wong, "Recent advances in noninvasive glucose monitoring," *Med. Devices: Evidence Res.*, vol. 5, p. 45, Jun. 2012, doi: 10.2147/mder.s28134.

[9] D. Bagchi and S. Nair, *Nutritional and Therapeutic Interventions for Diabetes and Metabolic Syndrome*. New York, NY, USA: Academic, 2018.

[10] T. Xu et al., "Electrospun CuO-nanoparticles-modified polycaprolactone @Polypyrrole fibers: An application to sensing glucose in saliva," *Nanomaterials*, vol. 8, no. 3, p. 133, Feb. 2018, doi: 10.3390/nano8030133.

[11] M. Nayak, S. Gupta, J. Sunitha, G. Dawar, N. Sinha, and N. Rallan, "Correlation of salivary glucose level with blood glucose level in diabetes mellitus," *J. Oral Maxillofacial Pathol.*, vol. 21, no. 3, p. 334, Dec. 2017, doi: 10.4103/jomfp.jomfp_222_15.

[12] R. Sha, L. Durai, and S. Badhulika, "Facile in-situ preparation of few-layered reduced graphene oxide—Niobium pentoxide composite for non-enzymatic glucose monitoring," in *Proc. 4th IEEE Int. Conf. Emerg. Electron. (ICEE)*, Dec. 2018, pp. 1–4, doi: 10.1109/ICEE44586.2018.8937860.

[13] K. P. Swain, G. Palai, M. V. S. V. Prasad, J. Sahoo, and J. K. Moharana, "Realization of accurate urine-glucose sensor using triangular photonic crystal structure," in *Proc. Int. Conf. Signal Process., Commun., Power Embedded Syst. (SCOPES)*, Oct. 2016, pp. 1021–1024, doi: 10.1109/SCOPES.2016.7955595.

[14] R. D. Munje, S. Muthukumar, and S. Prasad, "Lancet-free and label-free diagnostics of glucose in sweat using zinc oxide based flexible bioelectronics," *Sens. Actuators B, Chem.*, vol. 238, pp. 482–490, Jan. 2017, doi: 10.1016/j.snb.2016.07.088.

[15] Y. Wang, X. Wang, W. Lu, Q. Yuan, Y. Zheng, and B. Yao, "A thin film polyethylene terephthalate (PET) electrochemical sensor for detection of glucose in sweat," *Talanta*, vol. 198, pp. 86–92, Jun. 2019, doi: 10.1016/j.talanta.2019.01.104.

[16] Vinita, N. R. Nirala, M. Tiwari, and R. Prakash, "A nanoporous palladium(II) bridged coordination polymer acting as a peroxidase mimic in a method for visual detection of glucose in tear and saliva," *Microchimica Acta*, vol. 185, no. 4, p. 245, Apr. 2018, doi: 10.1007/s00604-018-2776-8.

[17] A. E. Kownacka et al., "Clinical evidence for use of a noninvasive biosensor for tear glucose as an alternative to painful finger-prick for diabetes management utilizing a biopolymer coating," *Biomacromolecules*, vol. 19, no. 11, pp. 4504–4511, Nov. 2018, doi: 10.1021/acs.biomac.8b01429.

[18] J. T. Baca, D. N. Finegold, and S. A. Asher, "Tear glucose analysis for the noninvasive detection and monitoring of diabetes mellitus," *Ocular Surf.*, vol. 5, no. 4, pp. 280–293, Oct. 2007, doi: 10.1016/s1542-0124(12)70094-0.

[19] J. Brunmair et al., "Metabolic phenotyping of tear fluid as a prognostic tool for personalised medicine exemplified by T2DM patients," *EPMA J.*, vol. 13, no. 1, pp. 107–123, Jan. 2022, doi: 10.1007/s13167-022-00272-7.

[20] D. Harvey, N. W. Hayes, and B. Tighe, "Fibre optics sensors in tear electrolyte analysis: Towards a novel point of care potassium sensor," *Contact Lens Anterior Eye*, vol. 35, no. 3, pp. 137–144, Jun. 2012, doi: 10.1016/j.clae.2012.02.004.

[21] D. Bruen, C. Delaney, L. Florea, and D. Diamond, "Glucose sensing for diabetes monitoring: Recent developments," *Sensors*, vol. 17, no. 8, p. 1866, Aug. 2017, doi: 10.3390/s17081866.

[22] J. C. Claussen et al., "Nanostructuring platinum nanoparticles on multilayered graphene petal nanosheets for electrochemical biosensing," *Adv. Funct. Mater.*, vol. 22, no. 16, pp. 3399–3405, Aug. 2012, doi: 10.1002/adfm.201200551.

[23] Q. Yan, B. Peng, G. Su, B. E. Cohan, T. C. Major, and M. E. Meyerhoff, "Measurement of tear glucose levels with amperometric glucose biosensor/capillary tube configuration," *Anal. Chem.*, vol. 83, no. 21, pp. 8341–8346, Nov. 2011, doi: 10.1021/ac201700c.

[24] C. J. Wan, Y. H. Liu, L. Q. Zhu, P. Feng, Y. Shi, and Q. Wan, "Short-term synaptic plasticity regulation in solution-gated indium–gallium–zinc-oxide electric-double-layer transistors," *ACS Appl. Mater. Interface*, vol. 8, no. 15, pp. 9762–9768, Apr. 2016, doi: 10.1021/acsami.5b12726.

[25] Y. S. Rim et al., "Printable ultrathin metal oxide semiconductor-based conformal biosensors," *ACS Nano*, vol. 9, no. 12, pp. 12174–12181, Dec. 2015, doi: 10.1021/acsnano.5b05325.

[26] *High-Density Carrier-Accumulated and Electrically Stable Oxide Thin-Film Transistors From Ion-Gel Gate Dielectric | Scientific Reports*. Accessed: Jun. 10, 2025. [Online]. Available: https://www.nature.com/articles/srep18168

[27] C. Hwang, Y. Song, S. Baek, J.-G. Choi, and S. Park, "Dual-biased metal oxide electrolyte-gated thin-film transistors for enhanced protonation in complex biofluids," *Sci. Rep.*, vol. 14, no. 1, p. 30772, Dec. 2024, doi: 10.1038/s41598-024-80005-0.

[28] C. Hwang, J. H. Lee, D.-K. Kim, K.-S. Na, and D. Y. Kim, "Real-time and highly sensitive detection of matrix metalloproteinase 9 (MMP-9) in tears using aptamer functionalized electrolyte-gated IGZO thin-film transistors," Tech. Rep., 2025.

[29] X. Xia et al., "Fabrication of metal oxide nanobranches on atomic-layer-deposited $TiO_2$ nanotube arrays and their application in energy storage," *Nanoscale*, vol. 5, no. 13, pp. 6040–6047, Jun. 2013, doi: 10.1039/c3nr01606d.

[30] S. Gora et al., "Asymmetric resistive switching by anion out-diffusion mechanism in transparent Al/ZnO/ITO heterostructure for memristor applications," *Surf. Interface*, vol. 30, Jun. 2022, Art. no. 101950, doi: 10.1016/j.surfin.2022.101950.

[31] R. A. Rodriguez-Davila, I. Mejia, R. A. Chapman, C. D. Young, and M. Quevedo-Lopez, "Performance and reliability comparison of ZnO and IGZO thin-film transistors and inverters fabricated at a maximum process temperature of 115 °C," *IEEE Trans. Electron Devices*, vol. 66, no. 9, pp. 3861–3866, Sep. 2019, doi: 10.1109/TED.2019.2931635.

[32] Y. S. Rim et al., "Interface engineering of metal oxide semiconductors for biosensing applications," *Adv. Mater. Interface*, vol. 4, no. 10, May 2017, Art. no. 1700020, doi: 10.1002/admi.201700020.

[33] J.-C. Chou et al., "The characteristic analysis of IGZO/Al pH sensor and glucose biosensor in static and dynamic measurements," *IEEE Sensors J.*, vol. 16, no. 23, pp. 8509–8516, Dec. 2016, doi: 10.1109/JSEN.2016.2609605.

[34] C. Hwang, T. Kwak, C.-H. Kim, J. H. Kim, and S. Park, "Quantitative and rapid detection of iodide ion via electrolyte-gated IGZO thin-film transistors," *Sens. Actuators B, Chem.*, vol. 353, Feb. 2022, Art. no. 131144, doi: 10.1016/j.snb.2021.131144.

[35] C. Hwang, S. Baek, Y. Song, W.-J. Lee, and S. Park, "Wide-range and selective detection of SARS-CoV-2 DNA via surface modification of electrolyte-gated IGZO thin-film transistors," *iScience*, vol. 27, no. 3, Mar. 2024, Art. no. 109061, doi: 10.1016/j.isci.2024.109061.

[36] S. Park et al., "Sub-0.5 v highly stable aqueous salt gated metal oxide electronics," *Sci. Rep.*, vol. 5, no. 1, p. 13088, Aug. 2015, doi: 10.1038/srep13088.

[37] A. Song et al., "Control of sensitivity in metal oxide electrolyte gated field-effect transistor-based glucose sensor by electronegativity modulation," *Sci. Rep.*, vol. 14, no. 1, p. 27251, Nov. 2024, doi: 10.1038/s41598-024-76885-x.

[38] D.-H. Kang et al., "Aqueous electrolyte-gated solution-processed metal oxide transistors for direct cellular interfaces," *APL Bioeng.*, vol. 7, no. 2, Apr. 2023, Art. no. 026102, doi: 10.1063/5.0138861.

[39] D. Bhatt, S. Kumar, and S. Panda, "Amorphous IGZO field effect transistor based flexible chemical and biosensors for label free detection," *Flexible Printed Electron.*, vol. 5, no. 1, Feb. 2020, Art. no. 014010, doi: 10.1088/2058-8585/ab724c.

[40] Y. Zhang et al., "Electrical detection assay based on programmable nucleic acid probe for efficient single-nucleotide polymorphism identification," *ACS Sensors*, vol. 8, no. 5, pp. 2096–2104, May 2023, doi: 10.1021/acssensors.3c00453.

[41] S. Udomsom, U. Mankong, P. Paengnakorn, and N. Theera-Umpon, "Novel rapid protein coating technique for silicon photonic biosensor to improve surface morphology and increase bioreceptor density," *Coatings*, vol. 11, no. 5, p. 595, May 2021, doi: 10.3390/coatings11050595.

[42] H. Shimotani, H. Asanuma, A. Tsukazaki, A. Ohtomo, M. Kawasaki, and Y. Iwasa, "Insulator-to-metal transition in ZnO by electric double layer gating," *Appl. Phys. Lett.*, vol. 91, no. 8, Aug. 2007, Art. no. 082106, doi: 10.1063/1.2772781.

[43] E. Said, X. Crispin, L. Herlogsson, S. Elhag, N. D. Robinson, and M. Berggren, "Polymer field-effect transistor gated via a poly(styrenesulfonic acid) thin film," *Appl. Phys. Lett.*, vol. 89, no. 14, Oct. 2006, Art. no. 143507, doi: 10.1063/1.2358315.

[44] J. L. Arlett, E. B. Myers, and M. L. Roukes, "Comparative advantages of mechanical biosensors," *Nature Nanotechnol.*, vol. 6, no. 4, pp. 203–215, Apr. 2011, doi: 10.1038/nnano.2011.44.

[45] C. Liao, M. Zhang, L. Niu, Z. Zheng, and F. Yan, "Highly selective and sensitive glucose sensors based on organic electrochemical transistors with graphene-modified gate electrodes," *J. Mater. Chem. B*, vol. 1, no. 31, p. 3820, 2013, doi: 10.1039/c3tb20451k.

[46] T. Healy, "Site-binding model of the electrical double layer at the oxide/water interface," Tech. Rep., 1974.

[47] D. K. Sen and G. S. Sarin, "Tear glucose levels in normal people and in diabetic patients," *Brit. J. Ophthalmol.*, vol. 64, no. 9, pp. 693–695, Sep. 1980.

[48] C.-P. Chen et al., "Ultrasensitive in situ label-free DNA detection using a GaN nanowire-based extended-gate field-effect-transistor sensor," *Anal. Chem.*, vol. 83, no. 6, pp. 1938–1943, Mar. 2011, doi: 10.1021/ac102489y.

[49] Y. Ohashi et al., "Abnormal protein profiles in tears with dry eye syndrome," *Amer. J. Ophthalmol.*, vol. 136, no. 2, pp. 291–299, Aug. 2003, doi: 10.1016/s0002-9394(03)00203-4.

[50] P. Velos, P. M. H. Cherry, and D. Miller, "An improved method for measuring human tear lysozyme concentration," *Arch. Ophthalmol.*, vol. 103, no. 1, pp. 31–33, Jan. 1985, doi: 10.1001/archopht.1985.01050010035012.

**Chuljin Hwang** received the Ph.D. degree in pharmacy from Ajou University, Suwon, South Korea, in 2022.

He is currently a Post-Doctoral Fellow Researcher with the Department of Electrical and Computer Engineering, Inha University, Incheon, Republic of Korea. His main research interests include oxide electronics, bioelectronic devices, microneedle, and so on.

**Sungjun Park** received the Ph.D. degree from Gwangju Institute of Science and Technology, Gwangju, South Korea, in 2017.

He is currently an Assistant Professor with the Department of Electrical and Computer Engineering, Ajou University, Suwon, South Korea. His main research interests include organic photovoltaics, skin-conformal bioelectronics, oxide electronics, and so on.

**Dae Yu Kim** received the B.S. degree in electrical engineering from Inha University, Incheon, South Korea, in 2000, the M.S. degree in electrical engineering from University at Buffalo, State University of New York (SUNY Buffalo), Buffalo, NY, USA, in 2007, and the Ph.D. degree in biomedical engineering from the University of California, Davis, CA, USA, in 2011.

He was a Med-into-Grad Scholar with the Howard Hughes Medical Institute, University of California. From 2012 to 2013, he was a Post-Doctoral Scholar with the Biological Imaging Center, Beckman Institute, California Institute of Technology, Pasadena, CA, USA. He is currently a Professor with the Department of Electrical and Computer Engineering, Inha University.